Journal of Magnetic Resonance 199 (2009) 238–241

Contents lists available at ScienceDirect

Journal of Magnetic Resonance

journal homepage: www.elsevier.com/locate/jmr

Communication

Low-power decoupling at high spinning frequencies in high static fields

Markus Weingarth, Geoffrey Bodenhausen, Piotr Tekely *

Département de Chimie, associé au CNRS, Ecole Normale Supérieure, 24 rue Lhomond, 75231 Paris Cedex 05, France

ARTICLE INFO

Article history:
Received 17 March 2009
Revised 23 April 2009
Available online 3 May 2009

Keywords:
Low-power heteronuclear decoupling
Fast MAS

ABSTRACT

We demonstrate that heteronuclear decoupling using a *P*hase-*I*nverted *S*upercycled *S*equence for *A*ttenuation of *R*otary *Res*O*n*ance (PISSARRO) is very efficient at high spinning frequencies (ν_{rot} = 60 kHz) and high magnetic fields (900 MHz for protons at 21 T) even with moderate radio-frequency decoupling amplitudes ($\nu_1{}^I$ = 15 kHz), despite the wide range of isotropic chemical shifts of the protons and the increased effect of their chemical shift anisotropy.

1. Introduction

Recently, a novel heteronuclear decoupling scheme dubbed PISSARRO (*P*hase-*I*nverted *S*upercycled *S*equence for *A*ttenuation of *R*otary *Res*O*n*ance) [1] was demonstrated to be efficient over a wide range of amplitudes $\nu_1{}^I$ of the radio-frequency (*rf*) field applied to the protons *I*. Initial trials were conducted at moderate spinning frequencies (30 kHz) and medium static fields (400 MHz for protons at 9.4 T). Under these conditions, PISSARRO decoupling proved to be more effective in quenching rotary resonance effects than established methods such as XiX [2,3], TPPM [4] or SPINAL-64 [5]. In particular, these conventional decoupling methods suffer from destructive interference due to rotary resonance effects, i.e., when $\nu_1{}^I \approx n\nu_{rot}$ with n = 1, 2, 3…. The interference of spinning and decoupling leads to undesirable line-broadening over wide ranges of *rf* amplitudes $\nu_1{}^I$, which is particularly annoying at high spinning frequencies ν_{rot} > 30 kHz. For CW decoupling with ν_{rot} = 40 kHz, rotary resonance effects broaden the lines of CH and CH_2 groups unless $\nu_1{}^I$ > 200 kHz [6] while for ν_{rot} = 70 kHz, such interference effects only disappear if $\nu_1{}^I$ > 300 kHz [7]. Thus it would seem that conventional decoupling methods would necessitate the use of ever increasing *rf* amplitudes with increasing spinning frequencies. Fortunately, it has been shown recently that it is also possible to use decoupling methods such as CW, XiX, and TPPM with much lower *rf* amplitudes $\nu_1{}^I << \nu_{rot}$, provided that ν_{rot} > 40 kHz [6,8,9]. The efficiency of decoupling with such low *rf* amplitudes is comparable to what can be achieved with high *rf* amplitudes $\nu_1{}^I >> \nu_{rot}$. This Communication shows that at high spinning frequencies (ν_{rot} = 60 kHz) and high static fields (900 MHz for protons at 21 T), PISSARRO decoupling remains remarkably efficient at commonly used *rf* amplitudes (~100 kHz). Even with a much lower *rf* amplitude $\nu_1{}^I$ = 15 kHz, PISSARRO performs just as well as high-power decoupling for CH_3 and CH signals. For the more challenging CH_2 groups, which have strong dipolar proton–proton couplings, low-amplitude PISSARRO with $\nu_1{}^I$ = 15 kHz leads to a mere 20% loss in peak height compared to $\nu_1{}^I$ = 150 kHz. This permits a dramatic reduction of the *rf* power dissipation in the sample, which is vital for heat-sensitive samples such as hydrated proteins with high salt content.

2. Experimental

The PISSARRO sequence is composed of N pulse pairs $(\tau_p)_x(\tau_p)_{-x}$ followed by N pairs $(\tau_p)_y(\tau_p)_{-y}$ that together form a block. We shall use N = 5 throughout this work. The choice of N = 5 yields optimal performance for 20 < ν_{rot} < 60 kHz. Four such blocks are combined to form a supercycle [1]. There is only a single adjustable parameter, i.e., the pulse width τ_p, or, equivalently, the ratio τ_p/τ_{rot}, where the rotor period is $\tau_{rot} = 1/\nu_{rot}$.

Polycrystalline powders of uniformly ^{13}C, ^{15}N labelled L-alanine and $^{13}C^{\alpha}$ labelled L-glycine were used without further purification. All experiments were performed on a 900 MHz Bruker Avance II spectrometer with a double resonance CP/MAS probe using rotors with 1.3 mm outer diameter spinning at ν_{rot} = 60 kHz. Ramped cross polarization (CP) [10] and a simple excitation by a 90° pulse were used to record spectra of L-glycine and L-alanine, respectively. Numerical simulations of PISSARRO and CW decoupling were carried out with SPINEVOLUTION [11]. For L-alanine, a cluster comprising one $^{13}C^{\alpha}$ nucleus and six intramolecular protons with distances derived from the crystallographic structure as well as two additional protons from the neighborhood was considered in the simulations. The latter two protons were assumed to be on resonance, and the rotation of the methyl protons was assumed to be very fast.

* Corresponding author. Fax: +33 144 323 344.
E-mail address: Piotr.Tekely@ens.fr (P. Tekely).

1090-7807/$ - see front matter © 2009 Elsevier Inc. All rights reserved.
doi:10.1016/j.jmr.2009.04.015

3. Results and discussion

3.1. Quenching interference due to rotary resonance

The performance of CW and PISSARRO decoupling at ν_{rot} = 60 kHz MAS is compared in Fig. 1 for CH and CH_2 groups. In the regime $\nu_1^I >> \nu_{rot}$, CW decoupling suffers from recoupling effects due to rotary resonance $\nu_1^I \approx n\nu_{rot}$ (n = 1 and 2) [12] over a wide range of *rf* amplitudes. With PISSARRO, these interference effects almost completely disappear for CH and CH_3 groups (the latter are not shown in Fig. 1), even with moderate *rf* amplitudes $\nu_1^I \approx 100$ kHz. Compared to earlier observations at ν_{rot} = 30 kHz [1], the efficiency of PISSARRO with ν_{rot} = 60 kHz is particularly satisfying for CH_2 groups. The recommended ratios are τ_p/τ_{rot} = 0.305 for $\nu_1^I \approx \nu_{rot}$, τ_p/τ_{rot} = 0.197 for $\nu_1^I \approx 2\nu_{rot}$, and τ_p/τ_{rot} = 0.9 or 1.1 for higher *rf* amplitudes $\nu_1^I >> 2\nu_{rot}$. Half and full rotor periods should be avoided, i.e., $\tau_p/\tau_{rot} \neq k/2$ with integer k. These recommendations can be followed blindly, although an empirical optimization in the vicinity of the recommended ratios τ_p/τ_{rot} may provide a minor improvement in decoupling efficiency. In practice, the optimal ratio τ_p/τ_{rot} is nearly the same at ν_{rot} = 60 and 30 kHz, which obviously makes it easy to set up PISSARRO decoupling.

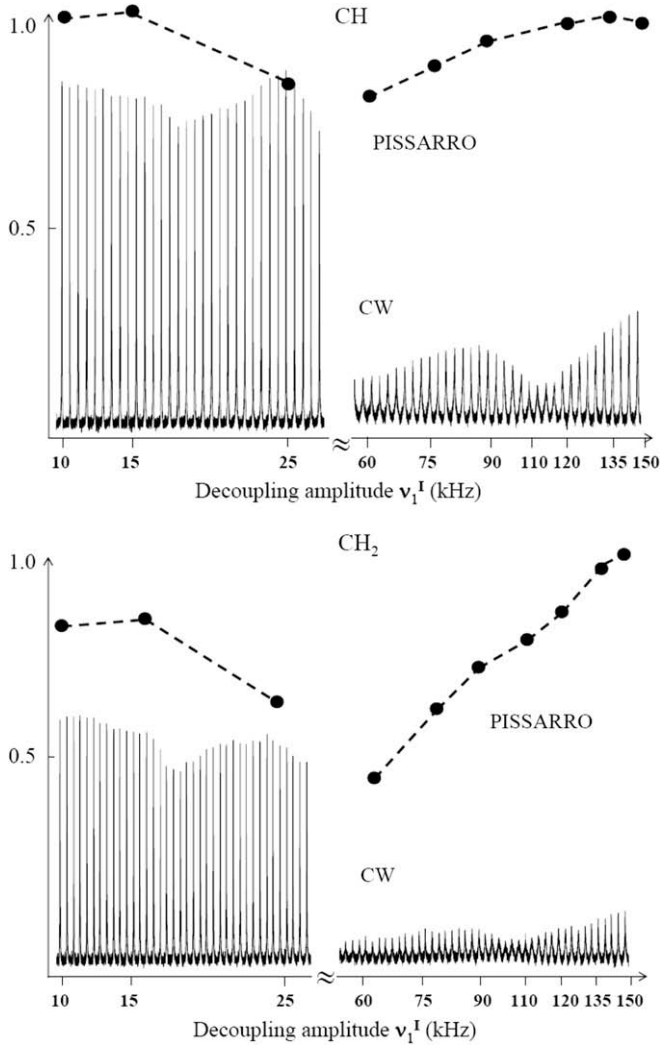

Fig. 1. Experimental intensities of the $^{13}C^{\alpha}H$ peak in L-alanine (top) and the $^{13}C^{\alpha}H_2$ resonance in L-glycine (below) as a function of the *rf* decoupling amplitude ν_1^I. All spectra were obtained on a 900 MHz spectrometer with ν_{rot} = 60 kHz. The signals obtained by CW decoupling are represented by continuous lines, the peak heights obtained with PISSARRO decoupling by circles.

As in earlier work [1], we noted for CH groups a significant 50% drop of the performance of XiX decoupling near the n = 1 rotary resonance condition, and a 30% drop near n = 2, in spite of careful optimization over a wide range of the pulse widths τ_p. For very high *rf* amplitudes, XiX and PISSARRO offer the same decoupling performance. PISSARRO reaches the best efficiency at lower *rf* amplitudes [1]. This is particularly important for CH_2 groups with strong dipolar proton–proton couplings, where low-amplitude decoupling might not be sufficient in certain applications (*vide infra*).

3.2. Low-amplitude decoupling

As shown in Figs. 1 and 2, PISSARRO decoupling is also remarkably efficient in the low-amplitude regime. For CH_3 and CH signals, despite a reduction of the *rf* power by a factor of 100, low-amplitude PISSARRO offered virtually the same decoupling performance as with the highest accessible amplitudes. On the other hand, the peak heights of CH_2 groups observed with ν_1^I = 15 kHz are only ~20% lower. Such a loss might be acceptable for heat-sensitive biological samples. We found the optimal performance of low-power PISSARRO to be uniform for all resonances with ν_1^I = 15 kHz when ν_{rot} = 60 kHz, i.e., with ν_1^I/ν_{rot} = 1/4. Nearly the same performance was observed with ν_1^I = 10 kHz. This stands in contrast to low-power CW decoupling, where the optimal decoupling amplitude differs from resonance to resonance.

The middle columns of Fig. 2 show a comparison between peakshapes recorded with ν_1^I = 15 and 25 kHz, the former corresponding to the optimal *rf* strength for low-amplitude PISSARRO for all resonances, and the latter to the best *rf* amplitude for CH resonances with CW decoupling. In all cases the lineshapes are affected by partially resolved ^{13}C–^{13}C J-couplings. This comparison reveals improvements of PISSARRO compared to CW decoupling of about 13%, 27%, and 35% in the peak heights of the CH_3, CH and CH_2 resonance signals, respectively. For the CH resonance, the linewidths for *rf* amplitudes of 150 and 15 kHz are 114 and 119 Hz, respectively, while CW decoupling at 25 kHz *rf* amplitude leads to a linewidth of 125 Hz. For the CH_2 resonance, the corresponding linewidths are 118, 128, and 144 Hz.

When using PISSARRO with low *rf* fields, the pulse length τ_p should be optimized so that the nutation angle $\beta = 2\pi\nu_1^I\tau_p$ is in the vicinity of a multiple of 2π (Fig. 3). Furthermore, in analogy to high-amplitude PISSARRO, half and full rotor periods should be avoided, i.e., $\tau_p/\tau_{rot} \neq k/2$ with integer k. However, compared to high-amplitude PISSARRO, the dips near the conditions $\tau_p/\tau_{rot} = k/2$ are less pronounced, which makes the sequence more robust with respect to minor misadjustments and instrumental instabilities.

To appreciate in more detail to what extent CW and PISSARRO decoupling are sensitive to resonance offsets and CSA of the irradiated spins, we carried out numerical simulations of low-amplitude decoupling. In all simulations, the spinning frequency was ν_{rot} = 60 kHz. In agreement with our experimental observations, the best performance of PISSARRO decoupling was found for ν_1^I = 15 kHz. The optimal pulse length τ_p corresponds to a ratio $\tau_{rot}/\tau_p \sim 3.86$, which is equivalent to a nutation angle $\beta \sim 349°$. This is in good agreement with the experimental observation that the optimal nutation angles should be in the vicinity of multiples of 2π For low-amplitude CW decoupling, the best performance was found for ν_1^I = 30 kHz, which roughly matches our experimental findings and relates to the so-called HORROR proton–proton recoupling condition $\nu_1^I = n\nu_{rot}$ with n = 1/2 [13]. Indeed, the resulting reintroduction of homonuclear couplings leads to a restoration of spin exchange in the proton network and improves the efficiency of CW decoupling in rotating solids [2,7].

Fig. 4a shows the height of the C^{α} peak in L-alanine as a function of the offset of the proton carrier from the isotropic shift of the H^{α}

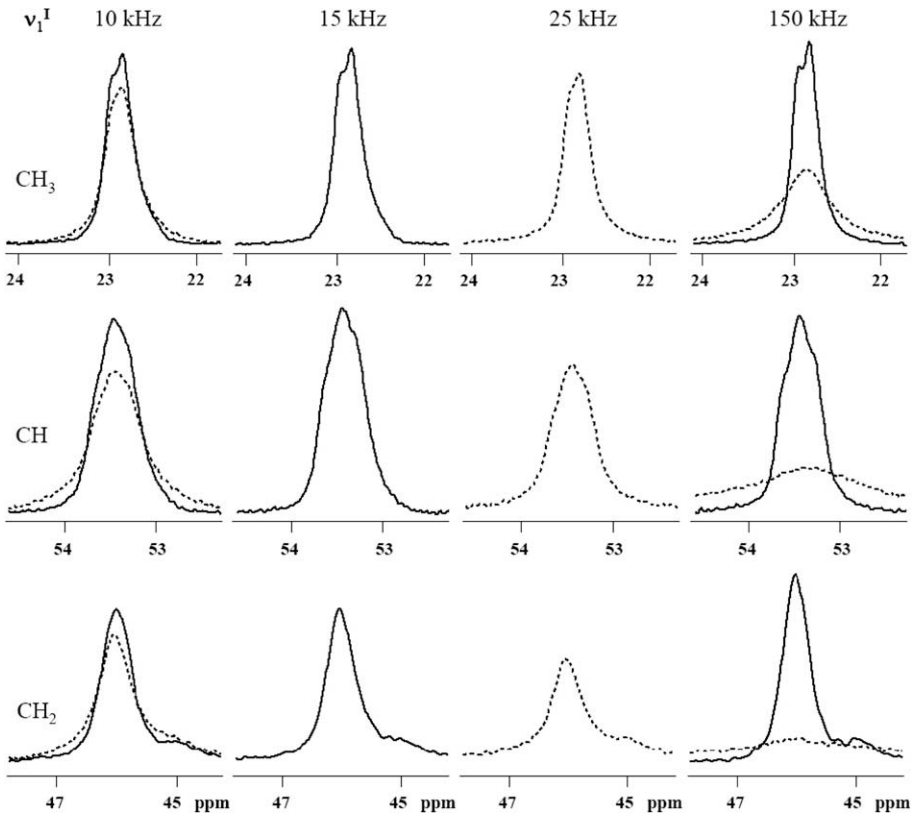

Fig. 2. Comparison of experimental peak-shapes of the $^{13}C^{\beta}H_3$ and $^{13}C^{\alpha}H$ peaks in L-alanine and the $^{13}C^{\alpha}H_2$ peak in L-glycine at different *rf* decoupling amplitudes $\nu_1{}^I$ = 10, 15, 25, and 150 kHz, using decoupling with PISSARRO (continuous lines) and CW (dotted lines) irradiation.

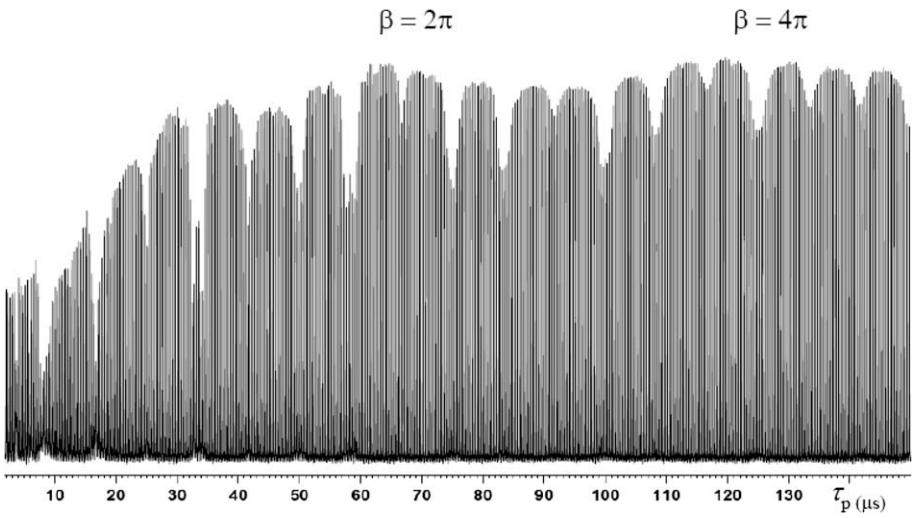

Fig. 3. Experimental $^{13}C^{\alpha}H$ signals of L-alanine obtained with low-amplitude PISSARRO decoupling with $\nu_1{}^I$ = 15 kHz as a function of the pulse width τ_p. Note the presence of dips due to undesired recoupling effects at multiples of half the rotor period, i.e., when $\tau_p/\tau_{rot} = k/2$ with integer k.

proton, simulated for two different static fields corresponding to 500 and 900 MHz. Fig. 4b shows simulations with and without CSA of the irradiated spin at 900 MHz. In contrast to PISSARRO, CW decoupling suffers from a pronounced offset dependence, even if the *rf* amplitude is twice as high. This leads to line-broadening and hence to a loss of peak height at high magnetic fields. The presence of amino H^N protons and H^{β} methyl protons as well as various residual homo- and heteronuclear dipolar couplings in L-alanine leads to the asymmetry in the responses of Fig. 4. In fact, because of stronger couplings between the C^{α} carbon and its directly attached H^{α} proton with the neighboring H^N protons than with the methyl protons, the broadening is less pronounced when the carrier frequency is displaced towards the H^N resonance. To the best of our knowledge, the implications of the offsets of neighboring protons have not been considered so far in the context of heteronuclear decoupling. A different type of off-resonance decoupling has been reported in calcium formate [14], which contains only a single proton species. In this case, the improved off-resonance decoupling was ascribed to a partial cancellation of higher-order cross-terms.

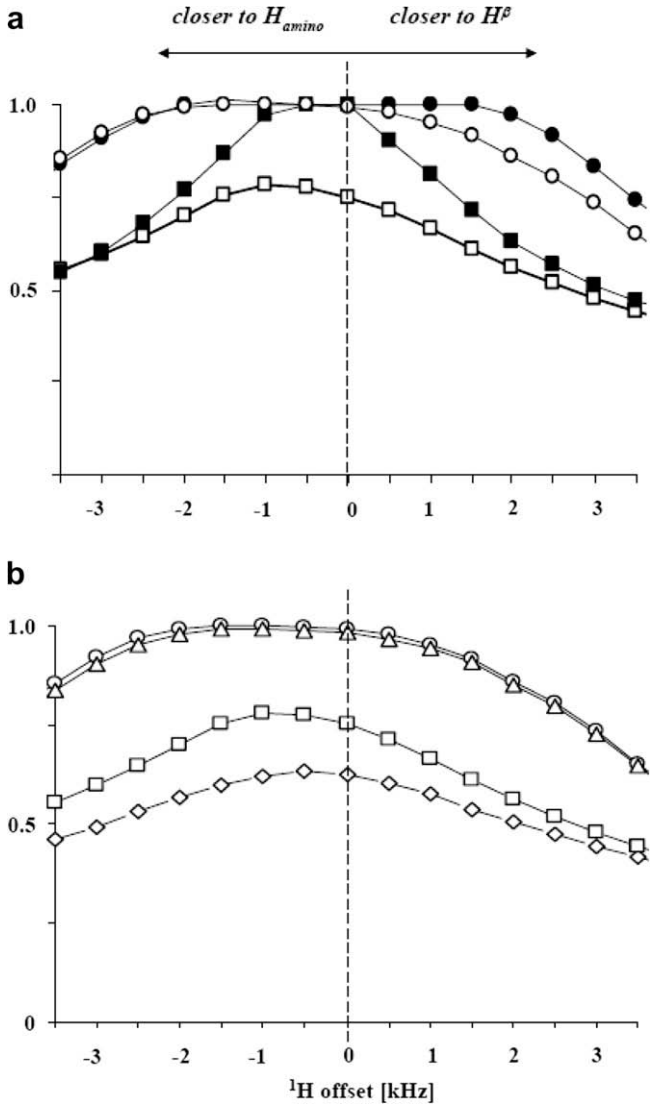

Fig. 4. (a) Numerical simulations of the $^{13}C^{\alpha}H$ peak heights in L-alanine as a function of the carrier frequency of the proton decoupler: (squares) low-amplitude CW decoupling ($\nu_1{}^I = 30$ kHz) and (circles) low-power PISSARRO decoupling ($\nu_1{}^I = 15$ kHz) at $\nu_{rot} = 60$ kHz. The filled and open symbols represent simulations for ^{1}H resonance frequencies of 500 and 900 MHz. (b) Simulations for low-amplitude CW decoupling (squares, lozenges) and low-power PISSARRO (circles, triangles) at 900 MHz, calculated without (squares, circles) and with (lozenges, triangles) a proton chemical shift anisotropy $\Delta\sigma = \sigma_{33} - \sigma_{iso} = 5$ ppm (4.5 kHz at 900 MHz). The peak heights were normalized with respect to the best performance of low-amplitude PISSARRO decoupling.

CW decoupling suffers from second-order recoupling effects due to cross-terms between the heteronuclear dipole–dipole and anisotropic chemical shielding interactions of the irradiated spins [15]. Indeed, as demonstrated in the simulations of Fig. 4b, low-amplitude CW decoupling is significantly affected by the CSA of the irradiated spins, while the efficiency of low-amplitude PISSARRO decoupling remains virtually unchanged. This is yet another reason why PISSARRO decoupling should be preferred at very high static fields.

4. Conclusions

We have shown that the most important feature of PISSARRO decoupling, i.e., its ability to quench interference effects due to rotary resonance, improves at high spinning frequencies. Because of the compensation of resonance offsets and of the chemical shift anisotropy of the irradiated spins, low-amplitude PISSARRO decoupling is particularly efficient at fast spinning in very high static fields.

Acknowledgments

The Research Infrastructure Activity in the 6th framework Program of the EU (contract No. RII3-026145, EU-NMR) and the European Center for High Field NMR in Lyon are greatly acknowledged. We thank P.K. Madhu and Michal Leskes for help with SPINEVOLUTION simulations.

References

[1] M. Weingarth, P. Tekely, B. Bodenhausen, Efficient heteronuclear decoupling by quenching rotary resonance in solid-state NMR, Chem. Phys. Lett. 466 (2008) 247–251.
[2] P. Tekely, P. Palmas, D. Canet, Effect of proton spin exchange on the residual ^{13}C MAS NMR linewidths, phase-modulated irradiation for efficient heteronuclear decoupling in rapidly rotating solids, J. Magn. Reson. A 107 (1994) 129–133.
[3] A. Detken, E.H. Hardy, M. Ernst, B.H. Meier, Simple and efficient decoupling in magic-angle spinning solid-state NMR: the XiX scheme, Chem. Phys. Lett. 356 (2002) 298–304.
[4] A.E. Bennett, C.M. Rienstra, M. Auger, K.V. Lakshli, R.G. Griffin, Heteronuclear decoupling in rotating solids, J. Chem. Phys. 103 (1995) 6951–6958.
[5] B.M. Fung, A.K. Khitrin, K. Ermolaev, An improved broadband decoupling sequence for liquid crystals and solids, J. Magn. Reson. 142 (2000) 97–101.
[6] M. Kotecha, N.P. Wickramasinghe, Y. Ishii, Efficient low-power heteronuclear decoupling in ^{13}C high-resolution solid-state NMR under fast magic angle spinning, Magn. Reson. Chem. 45 (2007) S221–S230.
[7] M. Ernst, A. Samoson, B.H. Meier, Decoupling and recoupling using continuous-wave irradiation in magic-angle-spinning solid-state NMR: a unified description using bimodal Floquet theory, J. Chem. Phys. 123 (2005) (064102-1-10).
[8] M. Ernst, A. Samoson, B.H. Meier, Low-power decoupling in fast magic-angle spinning NMR, Chem. Phys. Lett. 348 (2001) 293–302.
[9] M. Ernst, A. Samoson, B.H. Meier, Low-power XiX decoupling in MAS NMR experiments, J. Magn. Reson. 163 (2003) 332–339.
[10] G. Metz, X.L. Wu, S.O. Smith, Ramped-amplitude cross-polarization in magic-angle-spinning NMR, J. Magn. Reson. A 110 (1994) 219–227.
[11] M. Veshtort, R.G. Griffin, SPINEVOLUTION: a powerful tool for the simulation of solids and liquid state NMR experiments, J. Magn. Reson. 178 (2006) 248–282.
[12] T.G. Oas, R.G. Griffin, M.H. Levitt, Rotary resonance recoupling of dipolar interactions in solid-state nuclear magnetic resonance, J. Chem. Phys. 89 (1988) 692–695.
[13] N.C. Nielsen, H. Bildsoe, H.J. Jakobsen, M.H. Levitt, Double-quantum homonuclear rotary resonance. Efficient dipolar recovery in magic-angle spinning nuclear magnetic resonance, J. Chem. Phys. 101 (1994) 1805–1812.
[14] M. Eden, M.H. Levitt, Pulse sequence symmetries in the nuclear magnetic resonance of spinning solids: application to heteronuclear decoupling, J. Chem. Phys. 111 (1999) 1511–1519.
[15] M. Ernst, S. Bush, A.C. Kolbert, A. Pines, Second-order recoupling of chemical-shielding and dipolar-coupling tensors under spin decoupling in solid-state NMR, J. Chem. Phys. 106 (1996) 3387–3397.